JOURNAL OF MATERIALS SCIENCE 28 (1993) 469–476

Crystallization and properties of $CaO–P_2O_5–B_2O_3$ glasses

WEIDONG SHI, P. F. JAMES
Department of Engineering Materials, The University of Sheffield, Elmfield, Northumberland Road, Sheffield S10 2TZ, UK

Glasses were prepared with compositions $(50–0.5\ x)CaO.(50–0.5\ x)P_2O_5 \cdot x\ B_2O_3$ with B_2O_3 contents (x) from 0 to 45 mol%. The glass transformation temperature (T_g), dilatational softening temperature (T_D) and Vickers hardness (H_V) initially increased with x, but showed maxima at about $x=20$ for T_g and T_D and at about $x=35$ for H_V. The thermal expansion coefficient decreased with x, levelling off at about 35 mol% B_2O_3. The maximum tendency to crystallize occurred at around 25 mol% B_2O_3. Volume nucleation (and hence glass–ceramic formation) and surface nucleation were obtained for x between 15 and 25 mol%. The first phase to appear was BPO_4, which was probably homogeneously nucleated. Subsequently the $4CaO \cdot P_2O_5$ phase was heterogeneously nucleated on the BPO_4. For $10 \geqslant x \geqslant 35$ only surface nucleation was observed. The kinetics of nucleation were investigated in the 20 mol% B_2O_3 glass. The changes in properties and crystallisation behaviour with B_2O_3 content were related to short-range structural information. Infrared spectra and literature data indicated a three-dimensional network of B–O–B and B–O–P linkages in the glasses.

1. Introduction

In recent years there have been numerous studies of the nucleation and crystallization of silicate glasses and many glass–ceramics, materials prepared by the controlled crystallization of glasses, have been developed with a variety of properties and applications [1, 2]. However, there have been comparatively few investigations of possible glass–ceramic formation from calcium phosphate-based systems. These systems have potential applications in the medical and dental fields, for example for bone replacement or repair, because of their similar compositions to human hard tissues and their higher biocompatability than metals and many other ceramics [3–10]. Another potential application of phosphate glass–ceramics is in sealing to high thermal expansion metals [11]. Previous work has shown that it is difficult to promote volume (or bulk) crystal nucleation in phosphate glasses, although nucleation from the glass surface can be obtained fairly easily [5]. Recently Wang and James [12–14] found that addition of Al_2O_3, in combination with TiO_2 and SiO_2, promoted bulk nucleation in the $CaO–P_2O_5$ system. About 7 mol% Al_2O_3 was needed to produce, after heat treatment, high-volume nucleation of $AlPO_4$ crystals. These acted as heterogeneous nucleation sites for crystallization of the major calcium phosphate phase. In this way fine-grained glass–ceramics were produced in the $CaO–P_2O_5–SiO_2–Al_2O_3–TiO_2$ system containing around 40 mol% CaO and 40 mol% P_2O_5. Tests showed that these materials possessed good machinability.

In the present work crystallization was investigated in the $CaO–P_2O_5–B_2O_3$ system. The objects were to study the effects of B_2O_3 addition on the properties of $CaO–P_2O_5$ glasses and on their crystallization behaviour, including the possibility of forming glass–ceramics.

2. Experimental procedure

The glasses were prepared from reagent-grade calcium hydrogen phosphate, $CaH_4(PO_4)_2 \cdot H_2O$, and boric acid, H_3BO_3. The mole ratio CaO/P_2O_5 was kept equal to unity and the B_2O_3 content was varied from 0 to 45 mol% (Table I). The premixed batches were sintered first at 700 °C and were melted in alumina crucibles at 1200–1350 °C for 2 h. The melts were then poured on to a preheated graphite or steel plate. Glass samples for various property measurements were subsequently annealed at 560 to 590 °C for 2 h. Unannealed glass samples were given nucleation heat-treatments in a tube furnace. The nucleated samples were subsequently heat-treated at a higher temperature in a separate furnace to grow the nucleated crystals to observable dimensions. The growth temperature was chosen with the requirement that the nucleation rate was negligible at this temperature, and also that the growth rate was sufficient to enable the particles to be grown to an observable size in a convenient time. The microstructures of the heat-treated samples were observed in a Polyvar optical microscope. Specimens for transmission optical microscopy were ground on both sides to remove

0022–2461

TABLE I Compositions of $(50-0.5x)CaO\cdot(50-0.5x)P_2O_5\cdot xB_2O_3$ glasses

No.	CPB0	CPB1	CPB2	CPB3	CPB4	CPB5	CPB6	CPB7
x (mol %)	0	5	10	15	20	25	35	45

surface crystallization and reduced to a final thickness of 20 to 40 μm, using different grades of silicon carbide. The specimens for reflection optical microscopy were mounted on glass slides with Canada balsam, preground to remove surface crystallization, polished with cerirouge, and etched for up to 45 s in a $2HF\cdot2HCl\cdot96H_2O$ (vol %) solution. Nucleation densities, as determined by the number of crystal spherulites per unit volume, N_v, were obtained from optical micrographs of the polished and etched surfaces of the samples given the two-stage nucleation and growth heat-treatments. The optical micrographs, which corresponded to random plane sections through the glass samples, were analysed by the standard method of Dehoff and Rhines [15] using measurements of the number of spherulites per unit area of the section and the mean value of the reciprocals of the spherulite diameters. Application of this method to bulk nucleated glasses has been discussed by James [16].

Differential thermal analysis (DTA) was carried out using a Stanton Redcroft DTA-673 apparatus at a heating rate of 10 °C min^{-1}. The glass sample, in the form of 100 mg of powder ground to less than 150 μm, and the calcined alumina reference material were contained in platinum crucibles.

The linear coefficients of thermal expansion of the glasses were measured by a method in which the elongation of the sample was compared with that of silica glass. The sample was in the form of a rod 5 mm in diameter and 60 to 100 mm long, and the apparatus consisted of a platinum-wound furnace, a linear variable differential transducer (LVDT) and microcomputer. Measurements were made in the range 25 to 300 °C at a heating rate of 5 °C min^{-1}. The glass transition point (T_g) was determined from the change in slope of the elongation versus temperature plot. The dilatational softening temperature (T_D) was obtained from the position of the maximum on the expansion trace (Fig. 1). This results from the onset of viscous deformation of the glass sample, which is subjected to a small compressive force in the apparatus. The T_D values were apparatus-dependent and only useful for comparison between compositions.

The crystalline phases present after heat-treatment were identified by X-ray diffraction (XRD) using a Philips diffractometer with CuK_α radiation. For identification of the bulk phase, the samples were ground to remove the surface crystalline layers.

Infrared spectra of the glasses were obtained with a Perkin-Elmer 683 spectrophotometer and the KBr pellet technique. Specimens were prepared by mixing 200 mg KBr with 1 mg glass powder and the spectra were recorded in the wave number range of 4000 to 200 cm^{-1}.

Vickers hardness values were measured using a standard Leitz miniload hardness tester. A square sample of 20 mm × 20 mm with thickness of 10 mm was prepared for every composition. One surface was ground and polished to a mirror finish. With the specimen and diamond indenter, which was loaded with a different weight according to the experimental requirement in position (nearly touching), the indenter was released on to the specimen slowly. The whole process took about 15 s.

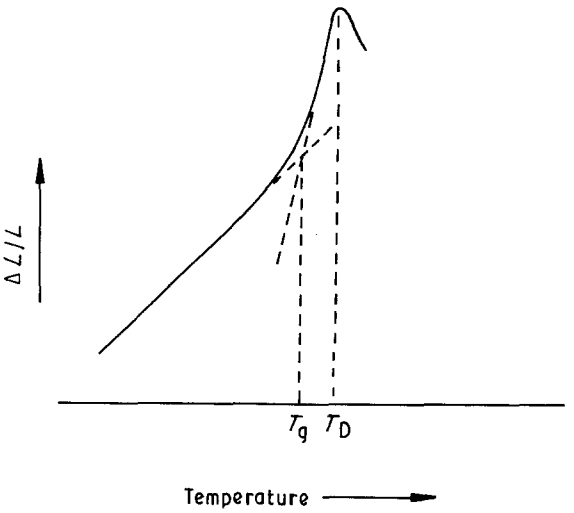

Figure 1 Thermal expansion trace of glass showing methods of determining glass transformation temperature (T_g) and dilatational softening temperature (T_D).

3. Results

3.1. Thermal and mechanical properties

The DTA traces for the eight glasses in the series $(50-0.5x)CaO\cdot(50-0.5x)P_2O_5\cdot xB_2O_3$ are shown in Fig. 2. The first endothermic dip corresponds to the glass transition, and the glass transformation temperature (T_g) was identified by a change in slope in the baseline of the curve using a standard method [17]. Each distinct exothermic peak on a trace probably corresponds to the appearance of a different crystalline phase. The endothermic dips at higher temperatures correspond to the melting of different phases. In this work the beginning of the highest-temperature endotherm observed was taken as a measure of the liquidus temperature. No further exothermic peaks or endothermic dips were observed for any of the glasses at temperatures up to 1200 °C, where the DTA runs were terminated. Fig. 3 shows the method used to determine the glass transformation temperature (T_g), peak crystallization temperature (T_c), melting endothermic dip temperature (T_m) and liquidus temperature (T_L). As can be seen from Fig. 2, the CPB2 trace (with 10 mol % B_2O_3) shows two exothermic crystallization peaks followed by three endothermic dips probably corresponding to the melting of different crystal phases, the highest corresponding to the liquidus from which T_L was determined. Two overlapping

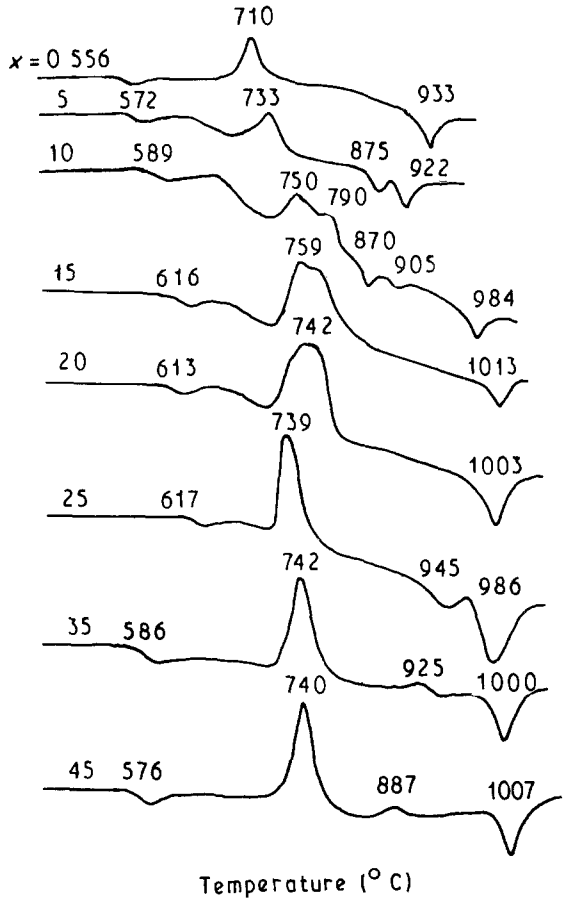

Figure 2 DTA traces of $(50-0.5x)CaO \cdot (50-0.5x)P_2O_5 \cdot xB_2O_3$ glasses using a heating rate of 10 °C min^{-1}. The highest and lowest temperatures recorded for each trace refer to T_L and T_g, respectively. The intermediate temperatures recorded correspond to the crystallization peaks (T_c) or melting dips (T_m). See Fig. 3 for further explanation.

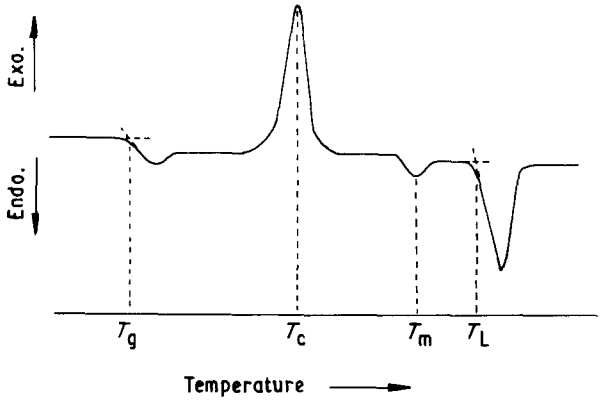

Figure 3 DTA curve showing methods of determining glass transformation temperature (T_g), peak crystallization temperature (T_c), melting dip temperature (T_m) and liquidus temperature (T_L).

exothermic peaks were observed in the traces of CPB3 (15 mol % B_2O_3) and CPB4 (20 mol % B_2O_3), but in each case only one endothermic dip at higher temperature was observed. The interpretation of the crystallization and melting phenomena was usually difficult, considerable overlap of the peaks often occurring.

The glass transformation temperatures obtained from thermal expansion traces were nearly the same as

TABLE II T_g and T_D obtained from DTA and thermal expansion curves

No.	T_g (°C) from DTA	T_g (°C) from thermal expansion	T_D (°C)
CPB0	556	–	–
CPB1	572	570	609
CPB2	589	586	625
CPB3	616	614	645
CPB4	613	610	645
CPB5	617	614	647
CPB6	586	584	620
CPB7	576	574	605

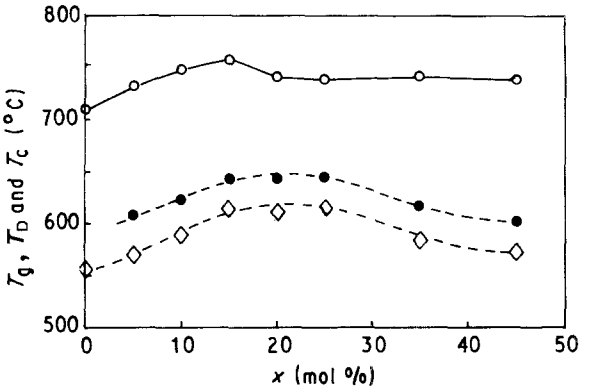

Figure 4 ◇ T_g, ● T_D and ○ T_c versus B_2O_3 content in $(50-0.5x)CaO \cdot (50-0.5x)P_2O_5 \cdot xB_2O_3$ glasses.

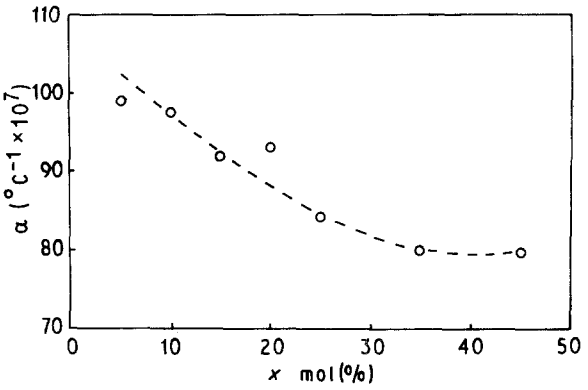

Figure 5 Thermal expansion coefficient (25 to 300 °C) versus x in $(50-0.5x)CaO \cdot (50-0.5x)P_2O_5 \cdot xB_2O_3$ glasses.

the values determined by DTA (Table II). Fig. 4 shows that T_g and T_D initially increase with increasing B_2O_3 content and reach a maximum at about 20 to 25 mol %. The peak crystallization temperature (T_c) increases with B_2O_3 content, reaching a maximum at about 15 mol % B_2O_3. With further B_2O_3 content T_c decreases and levels off above 20 mol %. The thermal expansion coefficient decreases with B_2O_3 content, levelling off (or possibly showing a minimum) at 35 mol % (Fig. 5). The Vickers hardness (H_V) (Fig. 6) initially shows an increase with B_2O_3 and a probable maximum at around 35 mol % B_2O_3.

3.2. Infrared transmission spectra

Infrared transmission spectra revealed short-range structural changes within the glasses. There were five

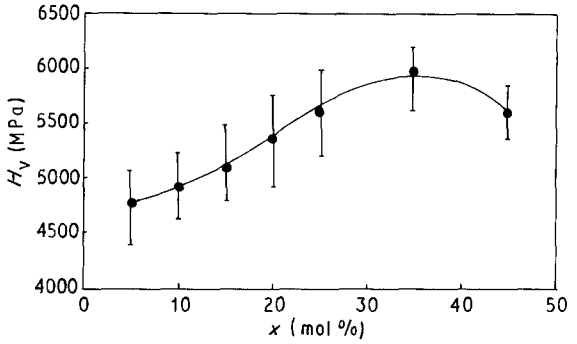

Figure 6 Microhardness H_V versus x in (50–0.5x)CaO·(50–0.5x) $P_2O_5 \cdot xB_2O_3$ glasses.

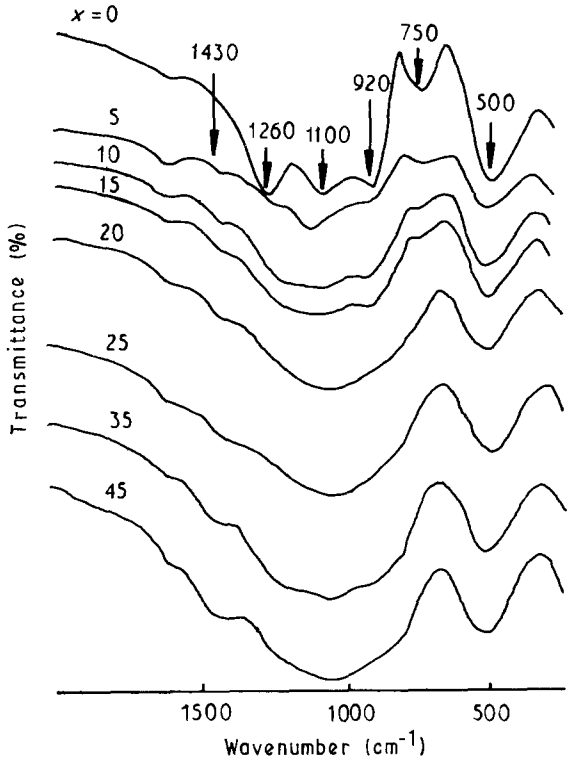

Figure 7 I.r. spectra obtained by the KBr pellet technique on powdered glass in (50–0.5x)CaO·(50–0.5x)$P_2O_5 \cdot xB_2O_3$ glasses. Transmittance scale arbitrary; traces separated for clarity of presentation.

distinct absorption bands in the infrared spectra (Fig. 7). The band at 500 cm^{-1} is associated with the bending of the O–P–O bond, while the band at 1260 cm^{-1} is related to the stretching vibration of the P=O bond [18]. The bands appearing at 1100, 920 and 750 cm^{-1} correspond to stretching vibrations of the P–O–P bond [18]. With increase of B_2O_3 content, all these bands except the bands at 500 and 1100 cm^{-1} became weaker, probably as a result of a decrease in the number of phosphorus–oxygen bonds. On the other hand, with the addition of B_2O_3 a new band appeared at 1430 cm^{-1} corresponding to the B–O–B vibration, indicating the presence of BO_3 or BO_4 groups [19]. The band at 500 cm^{-1} does not show a decrease in intensity with increase of B_2O_3 content. This may be explained if it is not only associated with bending of the O–P–O bond but also with the rocking motion of B–O–B linkages within the glassy network [20].

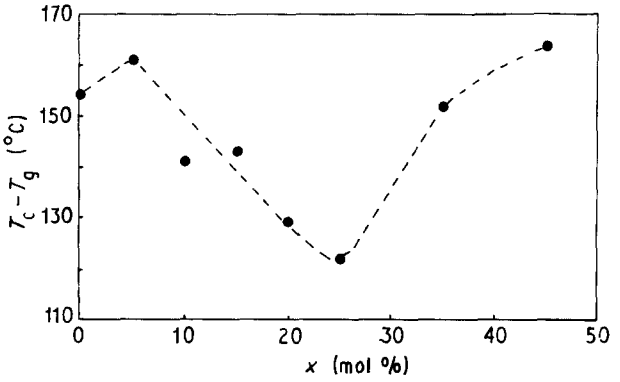

Figure 8 Glass-forming potential in (50–0.5x)CaO·(50–0.5x)$P_2O_5 \cdot xB_2O_3$ glasses by DTA, as assessed by $T_c - T_g$.

Figure 9 CPB1 glass heat-treated at 725 °C for 10 h. Optical transmission micrograph showing morphology of surface crystallization. Transmitted light normal to glass surface (bar denotes 50 μm).

3.3. Crystallization

All the glasses were heat-treated at a wide range of temperatures near T_g and above for different times to investigate the nucleation and crystallization behaviour. In Fig. 8, $T_c - T_g$, from DTA results is plotted against B_2O_3 content. $T_c - T_g$ can be used as a rough measure of the glass-forming ability of a composition [21], a lower value indicating a higher tendency towards crystallization. After a small initial increase for 5 mol % B_2O_3, the value of $T_c - T_g$ decreased with further B_2O_3 addition, reaching a minimum at around 25 mol %. This indicates an increasing crystallization tendency for B_2O_3 contents up to this value. When x was less than 15 mol %, only surface crystallization occurred even after heating for extended periods. A typical optical micrograph of surface crystallization is shown in Fig. 9. This micrograph was taken in transmitted light normal to the glass surface. The surface-precipitated crystals were identified as $4CaO \cdot P_2O_5$ by X-ray diffraction (Fig. 10a). When x was greater than 15 mol %, the glasses showed bulk (volume) crystallization. A low number-density of volume-nucleated crystal spherulites was observed in the glass CPB3 with 15 mol % B_2O_3 after heat-treatment in the range above T_g, as shown in Fig. 11. After removing the surface-crystallized layer, X-ray diffraction showed the presence of both the BPO_4 and $4CaO \cdot P_2O_5$ crystalline phases, indicating that the spherulites contained

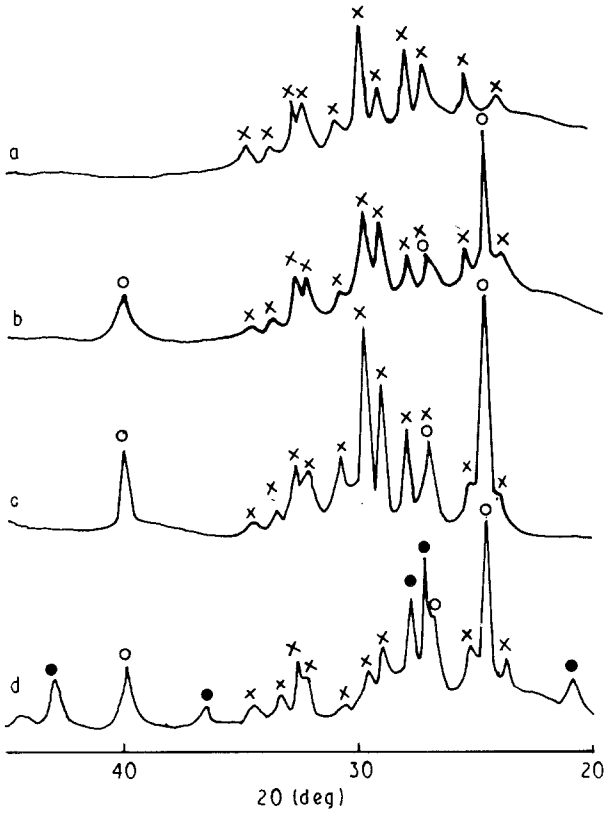

Figure 10 X-ray diffraction patterns for heat-treated glasses: (a) CPB1 at 725 °C for 10 h, (b) CPB3 at 725 °C for 10 h, (c) CPB4 at 610 °C for 2 h followed by 770 °C for 15 min, (d) CPB6 at 630 °C for 1 h followed by 680 °C for 10 h; (○) BPO_4, (×) $4CaO \cdot P_2O_5$, (●) α-$2CaO \cdot P_2O_5$.

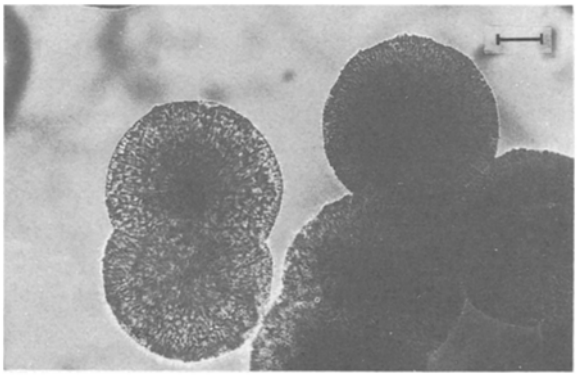

Figure 11 CPB3 glass heat-treated at 725 °C for 10 h. Optical transmission micrograph (bar denotes 50 μm).

both these phases (Fig. 10b). These phases were also detected in the surface-crystallized layer. Although glass CPB3 showed volume nucleation, various heat-treatments at different temperatures including two-stage heat treatments only produced a low number-density of spherulites, so that only a coarse microstructure of large crystal spherulites could be obtained.

In glasses CPB4 and CPB5 with B_2O_3 contents of 20 and 25 mol %, respectively, volume nucleation occurred more easily than in CPB3. Two-stage heat-treatments for CPB4 glass were conducted to study the kinetics of nucleation and crystallization. Figs 12–15 show the morphology of crystal spherulites after heat-treatment at 610 °C for different times

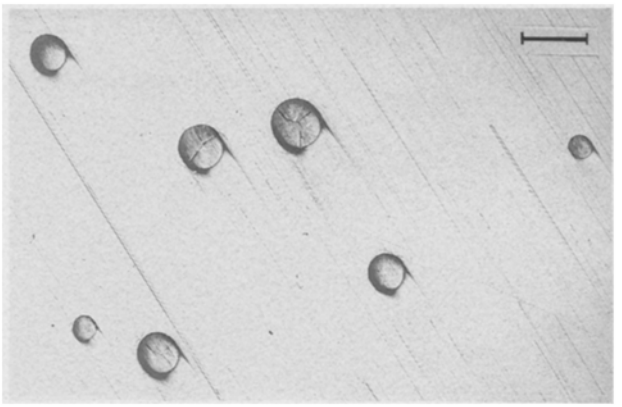

Figure 12 CPB4 glass heat-treated at 610 °C for 0.5 h (nucleation) followed by 770 °C for 15 min (growth treatment). Optical reflection micrograph of polished and etched section through glass sample (bar denotes 200 μm).

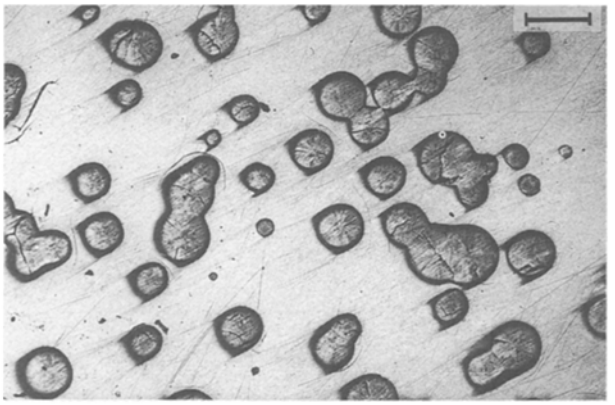

Figure 13 CPB4 glass heat-treated at 610 °C for 1 h (nucleation) followed by 770 °C for 15 min (growth). Optical reflection micrograph of polished and etched section through sample (bar denotes 200 μm).

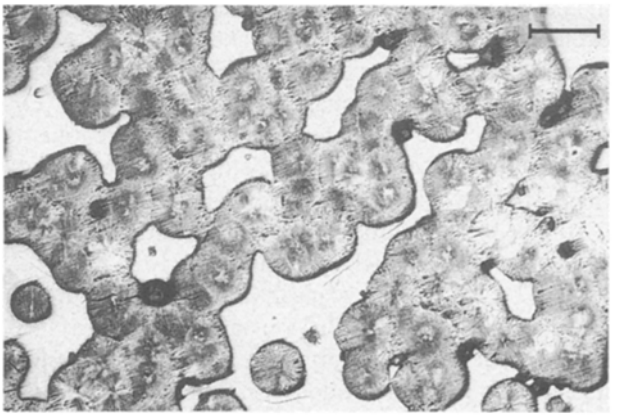

Figure 14 CPB4 glass heat-treated at 610 °C for 1.5 h (nucleation) followed by 770 °C for 15 min (growth). Optical reflection micrograph of polished and etched section through sample (bar denotes 200 μm).

using a constant growth treatment of 770 °C for 15 min. A significant increase in the number of spherulites per unit volume (N_v) was observed with time of the first-stage treatment at 610 °C, indicating that nucleation occurred at this temperature. The increase in N_v resulted in considerable overlap of spherulites

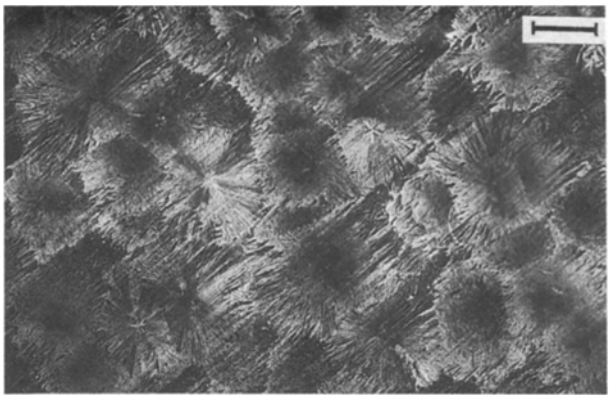

Figure 15 CPB4 glass heat-treated at 610 °C for 2 h (nucleation) followed by 770 °C for 15 min (growth). Optical reflection micrograph of polished and etched section through sample (bar denotes 100 μm).

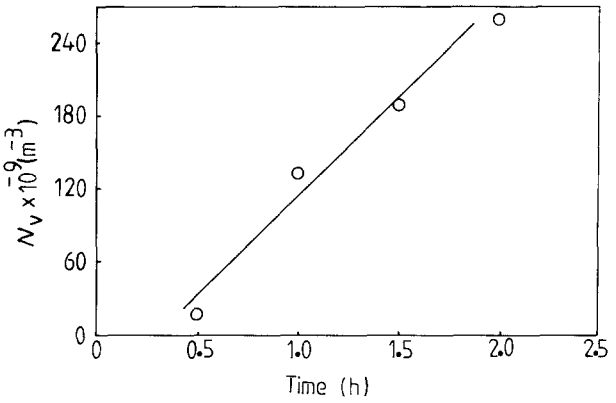

Figure 16 Crystal number density (N_v) versus time in CPB4 glass after nucleation at 610 °C for different times followed by growth treatment at 770 °C for 15 min.

for nucleation times of 1 h and over after the constant growth treatment (Figs 13–15). Subsidiary experiments at 770 °C showed that negligible nucleation occurred at this temperature. The X-ray diffraction pattern corresponding to Fig. 15 (Fig. 10c) showed the presence of the crystal phases BPO_4 and $4CaO \cdot P_2O_5$. Both phases were also detected for the heat-treatments used in Figs 12–14. For single-stage heat-treatments the first phase to be detected by XRD was BPO_4.

In Fig. 16 the number of spherulites per unit volume is plotted against nucleation time at 610 °C for glass CPB4. The N_v values were obtained from the micrographs shown in Figs 12–15 using the analysis mentioned earlier. The overlap of the spherulites at longer nucleation times introduced uncertainties in the N_v values obtained, but there is a clear increase in N_v with nucleation time. From the slope of the plot in Fig. 16, the steady-state nucleation rate was 4.3 $\times 10^7$ m^{-3} s^{-1}. The positive intercept with the time axis indicates the presence of a nucleation induction time as frequently observed in silicate systems [2, 16]. A more detailed study of the nucleation kinetics at different temperatures will be given in a later paper. In this glass the first phase to nucleate, BPO_4, was probably homogeneously nucleated. Subsequently the second phase $4CaO \cdot P_2O_5$ was heterogeneously nucleated on the BPO_4 phase.

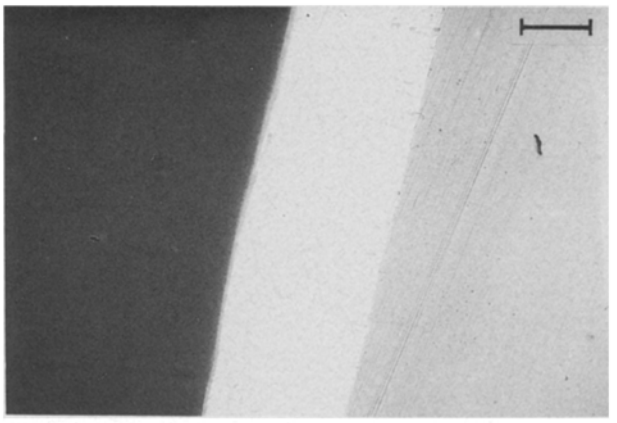

Figure 17 CPB6 glass heat-treated at 630 °C for 1 h followed by 680 °C for 10 h. Optical reflection micrograph of section normal to glass surface. Surface-crystallized layer is light region in centre, glass is region on right-hand side (bar denotes 100 μm).

The CPB5 glass showed similar crystallization behaviour to that of CPB4. The CPB6 glass (35 mol % B_2O_3) was heat-treated for a large range of temperatures for different periods of time but only surface crystallization was observed. A typical optical reflection micrograph is shown in Fig. 17. From XRD the precipitated phases were BPO_4, $4CaO \cdot P_2O_5$ and $\alpha 2CaO \cdot P_2O_5$ (see Fig. 10d). The presence of only surface crystallization in CPB6 indicates that crystallization is more difficult in this glass than in CPB5. This is consistent with the results in Fig. 8. When the B_2O_3 content was greater than 25 mol %, $T_c - T_g$ showed an increase, suggesting that the glass-forming tendency had increased or the tendency towards crystallization was reduced. For the CPB7 composition (45 mol % B_2O_3) an opalescent glass was obtained. The opalescence was attributed to liquid–liquid immiscibility since no crystallization was detected by XRD in as-prepared glass.

4. Discussion

The changes of thermal and mechanical properties with B_2O_3 content (Figs 4 to 6) probably reflect short-range structural changes in the glasses. The basic structural units of phosphate glasses are PO_4 tetrahedral units which are joined to form chains and rings, and it can be assumed that chains dominate [22, 23]. B_2O_3 is a network-former and two types of structural unit, BO_3 or BO_4, exist in borate glasses, corresponding to boron in three-or four-coordination with oxygen, respectively. Consequently, when B_2O_3 is added to a $CaO \cdot P_2O_5$ composition, the three structural units BO_3, BO_4 and PO_4 may be assumed to be present in the glass network.

The following suggested explanation of the effects of B_2O_3 on the structure of the glasses is based on previous studies of calcium and other borate glasses [24, 25]. For small B_2O_3 additions to the $CaO \cdot P_2O_5$ composition, BO_3 units are probably present consisting of either three or two non-bridging oxygens per boron atom. The former "orthoborate" group has been observed in the compound $3CaO \cdot B_2O_3$, while the latter "pyroborate" group has been observed in the

compound $2CaO \cdot B_2O_3$. For larger B_2O_3 contents the chain-type "metaborate" group with one non-bridging oxygen could be present, as found in the compound $CaO \cdot B_2O_3$. The formation of B–O–B bonds was indicated by the i.r. spectra. In addition these chain-type metaborate groups could form links with PO_4 chains. Indirect supporting evidence is provided by the crystallization results. Compositions with B_2O_3 contents of 15 to 25 mol % showed volume (probably homogeneous) nucleation of BPO_4 crystals, suggesting a tendency to form B–O–P linkages in the glass prior to crystallization heat-treatment. The maximum tendency towards BPO_4 nucleation occurred at around 25 mol % B_2O_3. Also, from the infrared spectra, the band at 1260 cm^{-1} related to the stretching vibration of the P=O double bond disappeared on adding B_2O_3, indicating destruction of P=O bonds and formation of links with boron atoms. Some BO_4-based groups in the glass may also form links with BO_3 or PO_4-based groups, although there is no supporting evidence at present. It may be speculated that BO_3 chain-type groups and BO_4-type groups are linked to PO_4 groups in a three-dimensional network containing B–O–B, P–O–P and B–O–P bonds.

Initially the increase in network-former (B_2O_3) and decrease in network-modifier (CaO) is expected to lead to a more rigid overall structure due to the larger proportion of stronger bonds in the glass. This probably accounts for the initial increase in thermal and mechanical properties (T_g, T_D and H_V) and decrease in expansion coefficient (α) with B_2O_3 addition. At higher B_2O_3 contents T_g, T_D and H_V reach maximum values and begin to decrease, whereas α levels off. These changes might reflect an eventual decrease in the number of B–O–P bonds, but an additional contributory effect could be a decrease in the number of BPO_4 groups in the glasses. At high B_2O_3 contents, BO_3 groups are expected to dominate in the glass network because all of the boron in the pure B_2O_3 glass is triangularly coordinated [25].

It appears that short-range structural changes in these glasses, particularly the presence of B–O–P linkages, in a general way account for the property variations and homogeneous nucleation of BPO_4. However, structural models of the property and nucleation behaviour will require more detailed information on all the structural groups, including BO_3, BO_4 and PO_4, as a function of B_2O_3 content using Raman and NMR studies.

5. Summary and conclusions

The properties and crystallization behaviour of glasses with compositions $(50–0.5x)CaO \cdot (50–0.5x)P_2O_5 \cdot xB_2O_3$ with x from 0 to 45 mol % were characterized by means of DTA, X-ray diffraction, optical microscopy, infrared spectroscopy, and measurements of hardness and thermal expansion. The glass transformation temperature (T_g) and dilatational softening temperature (T_D) initially increased with x and showed maxima at about 20 to 25 mol % B_2O_3. The peak crystallization temperature (T_c) from DTA reached a maximum at about 15 mol % B_2O_3. The thermal expansion coefficient (α) decreased with x, levelling off at about 35 mol % B_2O_3, while the Vickers hardness (H_V) initially showed an increase with x and a probable maximum at around 35 mol %.

The value of $T_c - T_g$ from DTA exhibited a minimum at about 25 mol % B_2O_3, indicating maximum tendency to crystallize at this composition. For x less than 15 mol % B_2O_3 only surface crystallization was observed. For x equal to 15 mol % both surface and volume (bulk) crystallization occurred, and the crystalline phases BPO_4 and $4CaO \cdot P_2O_5$ were identified by XRD. A low number-density of volume-nucleated spherulites was observed after heat-treatment in the temperature range above T_g. Volume nucleation occurred more easily in the 20 and 25 mol % B_2O_3 glasses, the volume nucleation rate of spherulites in the 20 mol % B_2O_3 glass being 4.3×10^7 m^{-3} s^{-1} at 610 °C. From XRD the first phase to appear was BPO_4 which was probably homogeneously nucleated. Subsequently the $4CaO \cdot P_2O_5$ phase appeared, probably heterogeneously nucleated on the BPO_4 crystals. In the 35 mol % B_2O_3 glass only surface crystallization was obtained. The phases detected were BPO_4, $4CaO \cdot P_2O_5$ and α-$2CaO \cdot P_2O_5$. Thus volume nucleation only occurred for the central range of compositions around 25 mol % B_2O_3.

The changes in properties and crystallization behaviour reflect short-range structural changes in the glasses. The infrared spectra indicate the formation of B–O–B bonds in the glasses on addition of B_2O_3. It is suggested that BO_3 units consisting of either three or two non-bridging oxygens per boron are present for small B_2O_3 additions, and that chain-type "metaborate" groups with one non-bridging oxygen occur at larger B_2O_3 additions. In addition B–O–P linkages are present, as indicated by the infrared spectra and the tendency to crystallize the BPO_4 phase, particularly at around 25 mol % B_2O_3.

The initial increase in thermal and mechanical properties (T_g, T_D and H_V) and the decrease in thermal expansion coefficient (α) may be explained by the increase in network-former (B_2O_3) and decrease in network-modifier (CaO), leading to a more rigid three-dimensional structure of stronger bonds in the glass. At higher B_2O_3 contents, the maxima in T_g, T_D and H_V and levelling off in α may partly reflect the eventual decrease in B–O–P bonds, but is probably a more complex function of the numbers of BO_3, BO_4 and PO_4-type groups present in the glasses.

Acknowledgement

W. Shi wishes to thank the Government of China and the British Council for financial support.

References

1. P. W. McMILLAN, "Glass Ceramics," 2nd Edn (Academic, London, 1979).
2. P. F. JAMES, in "Glasses and Glass Ceramics", edited by M. H. Lewis (Chapman and Hall, London, 1989) pp. 59–105.
3. M. AKAO, H. AOKI and K. KATO, *J. Mater. Sci.* **16** (1981) 809.

4. L. L. HENCH, in Proceedings of 10th International Congress on Glass, Kyoto, July 1974 (Ceramic Society of Japan, Tokyo) No. 9, p. 30.
5. Y. ABE and H. SAITO, *J. Jpn. Ceram. Soc.* **85** (1977) 45.
6. H. BROMER, K. DEUTSHER, B. BLENKÉ, E. PFEIL and V. STRUNZ, *Sci. Ceram.* **9** (1977) 219.
7. T. KOKUBO, S. ITO, M. SHIGEMATSU, S. SAKKA and T. YAMAMURO, *J.Mater. Sci.* **20** (1985) 2001.
8. T. NAKAMURA, T. YAMAMURO, S. HIGASHI, T. KOKUBO and S. ITO, *J. Biomed. Mater. Res.* **19** (985) 685.
9. J. VOGEL, W. HOLAND and W. VOGEL, US Patent 4 698 318 (1987).
10. A. OSAKA, Y. TOHO, M. ASADA and Y. MIURA, *Mater. Lett.* **6** (1988) 347.
11. J. A. WILDER Jr, J. T. HEALEY and B. C. BUNKER, in "Advances in Ceramics Vol 4", edited by J. H. Simmons, D. R. Uhlmann and G. H. Beall (American Ceramic Society, Columbus, Ohio, 1982) pp. 313–333.
12. P. F. JAMES, UK Patent 2 199 028 (1986).
13. T. H. WANG, PhD thesis, University of Sheffield (1987).
14. T. H. WANG and P. F. JAMES, in "New Materials and their Applications" edited by D. Holland, Conference Series No. 111 (Institute of Physics, Bristol, 1990), p. 401.
15. R. T. DEHOFF and F. N. RHINES, *Trans. Metall. Soc. AIME* **221** (1961) 975.
16. P. F. JAMES, *Phys. Chem. Glasses* **15** (1974) 95.
17. I. WOZNIAK and P. F. JAMES, *Glass Technol.* **25** (1984) 98.
18. J. WONG and C. A. ANGELL, "Glass Structure by Spectroscopy" (Dekker, New York, 1976) p. 864.
19. A. M. ABO-EL-AZM, I. KASHIF, H. FAROUK, A. M. SANAD and Y. M. ABO-ZEID, *Phys. Chem. Glasses* **30** (1989) 251.
20. R. M. ALMEIDA and J. D. MACKENZIE, *J. Non-Cryst. Solids* **40** (1980) 535.
21. C. A. ANGELL, in Proceedings of 2nd International Symposium on Halide Glasses, Rensselaer Polytechnic Institute, Troy, New York, 1983, Paper No. 8 (extended abstract).
22. A. E. R. WESTMAN, in "Modern Aspects of the Vitreous State I", edited by J. D. Mackenzie (1960) p. 63.
23. J. C. ARRIAGADA, W. BURCKHARDT and A. FELTY, *J. Non-Cryst. Solids* **91** (1987) 375.
24. W. L. KONIJNENDIJK and J. M. STEVELS, in "Borate Glasses", Materials Science Research Vol. 12, edited by L. D. Pye, V. D. Frechette and N. J. Kreidl (Plenum, New York, 1978) p. 259.
25. D. L. GRISCOM, *ibid.* p. 35.

Received 22 November 1991
and accepted 7 April 1992